Validation of Spectral Domain Optical Coherence Tomographic Doppler Shifts Using an In Vitro Flow Model

Larry Kagemann,[1,2] *Gadi Wollstein,*[1] *Hiroshi Ishikawa,*[1,2] *Kelly A. Townsend,*[1] *and Joel S. Schuman*[1,2,3]

Purpose. To validate velocity measurements produced by spectral domain optical coherence tomography (SD-OCT) in an in vitro laminar flow model.

Methods. A 30-mL syringe filled with skim milk was inserted into a syringe pump. Intravenous (IV) tubing connected the syringe within the pump to a glass capillary tube (internal diameter, 0.579 mm) shallowly embedded in agarose gel, then to a collection reservoir. SD-OCT imaging was performed with an anterior segment eye scanner and optics engine coupled with a 100-nm bandwidth broadband superluminescent diode. Scan density of 128 × 128 A-scans was spread over a 4 × 4 mm area, and each A-scan was 2 mm in length. Fifteen sequential stationary A-scans were obtained at each 128 × 128 position, and Doppler shifts were calculated from temporal changes in phase. The beam-to-flow vector Doppler angle was determined from three-dimensional scans.

Results. In all reflectance and Doppler images, a clear laminar flow pattern was observed, with v_{max} appearing in the center of the flow column. Phase wrapping was observed at all measured flow velocities, and fringe washout progressively shattered reflectance and phase signals beyond the Nyquist limit. The observed percentages of the velocity profile at or below Nyquist frequency was highly correlated with the predicted percentages ($R^2 = 0.934$; $P = 0.007$).

Conclusions. SD-OCT provides objective Doppler measurements of laminar fluid flow in an in vitro flow system in a range up to the Nyquist limit. (*Invest Ophthalmol Vis Sci.* 2009;50: 702–706) DOI:10.1167/iovs.08-2305

From the [1]UPMC Eye Center, Eye and Ear Institute, Ophthalmology and Visual Science Research Center, University of Pittsburgh School of Medicine, Pittsburgh, Pennsylvania; [2]Department of Bioengineering, Swanson School of Engineering, University of Pittsburgh, Pittsburgh, Pennsylvania; and [3]Center for the Neural Basis of Cognition, Carnegie Mellon University and University of Pittsburgh, Pittsburgh, Pennsylvania.

Presented in part at the annual meeting of the Association for Research in Vision and Ophthalmology, Fort Lauderdale, Florida, April 2008.

Supported by National Institutes of Health Grants R01-EY13178-08 and P30-EY008098; The Eye and Ear Foundation (Pittsburgh, PA); unrestricted grants from Research to Prevent Blindness; Carl Zeiss Meditec (GW); and Optovue (GW).

Submitted for publication May 17, 2008; revised July 2 and September 11, 2008; accepted December 8, 2008.

Disclosure: **L. Kagemann**, None; **G. Wollstein**, None; **H. Ishikawa**, None; **K.A. Townsend**, None; **J.S. Schuman**, Carl Zeiss Meditec (F), P

The publication costs of this article were defrayed in part by page charge payment. This article must therefore be marked "*advertisement*" in accordance with 18 U.S.C. §1734 solely to indicate this fact.

Corresponding author: Gadi Wollstein, UPMC Eye Center, Eye and Ear Institute, Ophthalmology and Visual Science Research Center, University of Pittsburgh School of Medicine, Suite 834, 203 Lothrop Street, Pittsburgh, PA 15213; wollsteing@upmc.edu.

Optical coherence tomography (OCT) is a ranging technique based on low-coherence interferometry, which has been applied to structural imaging of the eye.[1] Spectral domain OCT (SD-OCT) uses advances in broadband low-coherence light sources and high-speed linear array detector technologies, acquiring complete 1024 pixel A-scans in a single spectrometer measurement.[2,3] Reflectance intensities are frequency encoded in the raw SD-OCT fringe pattern. Fourier analysis of SD-OCT yields more than reflectance data. Doppler signals from all points within the reflectance data set are also produced and have recently been used to measure retinal blood flow.[4,5] The real (or power) component of the Fourier transform of SD-OCT data produces an A-scan, and Doppler measurements are contained in the imaginary (or phase) component.[5,6] However, the dynamic range of SD-OCT Doppler measurements is limited to low velocities by spectrometer limitations.

High velocities produce large Doppler shifts that physically manifest as rapid translation of the associated carrier frequency across the face of the spectrometer. Because of this, structural measurements of moving back-scattering sources and SD-OCT Doppler measurements are limited by the A-scan rate, which limits the ability of the charge-coupled device (CCD) to capture moving carrier waves without blur.[5] The purpose of the present study was to validate SD-OCT Doppler velocity measurements under well-controlled conditions in an in vitro laminar flow model.

Methods

Experimental Setup

A 30-mL syringe was filled with skim milk and inserted into a syringe pump (Perfusor Basic; B. Braun Medical, Bethlehem, PA). Flow rates were set in terms of the amount of time to empty the syringe. The slowest available settings were used in this experiment, keeping them within a range relevant to measurements in retinal vessels. Pump settings and resultant flow rates, mean velocities, and maximum velocities are listed in Table 1. Intravenous (IV) tubing connected the syringe within the pump to a glass capillary tube (internal diameter, 0.579 mm; Yankee 20λ disposable micropipette; Becton Dickinson, Parsippany, NJ) shallowly embedded in agarose gel. Intravenous tubing then carried the milk to a collection reservoir (Fig. 1). The orientation of the milk column within the three-dimensional (3D) scan data was used to determine the Doppler angle relative to the interrogating SD-OCT beam. All measurements were performed with the capillary tube in a single location, and the Doppler angle remained constant throughout the experiment.

All imaging was performed with a customized SD-OCT consisting of an anterior segment eye scanner and optics engine (Bioptigen, Research Triangle Park, NC) coupled with a 3-diode, 100-nm bandwidth broadband superluminescent diode (T-840; Superlum, Cork, Ireland). This configuration yielded a theoretical axial scan resolution of 3.5 μm in medium. CCD integration time was set at 35 μs, yielding an A-scan frequency of 28,571 Hz and a Nyquist limit of 14,285 Hz for Doppler

TABLE 1. Pump Flow Setting Results

Pump Setting (min/30 mL)	Flow Rate (mL/min)	Mean Velocity in Tube (mm/s)	Peak Velocity in Tube
55	0.55	35.0	70.0
50	0.6	38.5	77.0
45	0.67	42.8	85.6
40	0.75	48.1	96.2
35	0.86	55.0	110.0

Based on the volume of the capillary tube, pump settings produced these flow and velocity rates.

shifts. The velocity associated with this limit is a function of the center wavelength of the SD-OCT light source, the medium in which flow occurs, and the angle of the velocity vector relative to the SD-OCT beam[4] and is calculated as:

$$\text{Velocity} = \frac{\text{Doppler Frequency} \times \text{Center Wavelength}}{2 \times \text{Refractive Index} \times \text{Cos(Doppler Angle)}} \quad (1)$$

In water (refractive index, 1.33), and with velocity oriented perpendicularly into the beam (angle, 0; cosine(0), 1), an 870-nm centered light source sampled at 28,000 Hz has a Doppler velocity Nyquist limit of 4.58 mm/s.[4] Doppler shift measurements were recorded on a 16-bit scale. The center of the scale, 32,767, represents a Doppler shift of zero. Negative Doppler shifts were evenly distributed from 32,766 to 0, with 0 the negative Doppler Nyquist velocity. Positive Doppler shifts were evenly distributed from 32,768 to 65,535, with 65,535 the positive Nyquist Doppler limit. Thus, Figures 2 and 3 display Doppler samples with background noise fluctuating around 32,767 (0 Doppler). Doppler images were processed with ImageJ (1.38X; developed by Wayne Rasband, National Institutes of Health, Bethesda, MD; available at http://rsb.info.nih.gov/ij/index.html).

A density of 128 × 128 A-scans was spread over a 4 × 4 mm area, and each A-scan was 2 mm in length. Fifteen sequential stationary A-scans were obtained at each of the 128 × 128 positions, and Doppler shifts were calculated from temporal changes in phase.

Measurement Validation

The model produced laminar flow at well-controlled rates, which meant that the velocity throughout the tube was known because of the parabolic velocity distribution. Hence, it was possible to determine exactly where the velocity would surpass the upper limit of the measurement device. This location was calculated for each flow rate used in the experiment. The known and measured location of the Nyquist limit velocity within the flow profile was compared. Specifically, expected and observed proportions of usable signal at each flow level were compared by Wilcoxon signed-rank comparison (Fig. 4). Expected values were regressed against known values created by the model. $P < 0.05$ was considered statistically significant.

RESULTS

In all reflectance and Doppler images, a clear laminar flow pattern was observed, with v_{max} in the center of the flow column, an apparent parabolic velocity distribution in the "bull's-eye" pattern of the Doppler image, and the non-phase-wrapped portions of the cross-sectional velocity profiles. Phase wrapping was observed (Fig. 3).

Doppler Imaging and Flow Orientation

Clear, well-focused 3D reflectance and Doppler domain image sets were successfully recorded at mean flow speeds of 35.0, 38.5, 42.8, 48.1, and 55.0 mm/s.

The position of the fluid column relative to the scanning beam was determined by locating two points on the column in space: x_1, y_1, z_1 and x_2, y_2, z_2. Specifically, these points were identified on two different slices (x_1 and x_2; Fig. 5) widely spaced within the 3D data set. The length of the tangential component (Fig. 5) was calculated as

$$\text{Tangential} = \sqrt{(x_2 - x_1)^2 + (y_2 - y_1)^2} \quad (2)$$

and the measured component as $z_2 - z_1$. The angle between the beam and flow vector was equal to

$$\tan^{-1}\left(\frac{\text{Tangential}}{\text{measured}}\right). \quad (3)$$

Because the measured component of the flow vector was oriented away from the illuminating laser beam, Doppler shifts were negative. Reflectance within the flow column decreased with increasing velocity (Fig. 6).

Phase Wrapping

Phase wrapping was observed at all measured flow velocities. The Nyquist velocity, or location of phase wrap, was observed where the black Doppler velocity signal abruptly became white (Fig. 2). Velocity profiles were created at the Nyquist frequency (Fig. 2A) and through the center of the Doppler image (Fig. 2B). Smoothing (3 × 3 averaging kernel) of the Doppler image (Fig. 3) failed to produce a recognizable phase-wrap signal, as presented in the theoretical Figure 7.

Doppler Validation below Nyquist

There was no statistically significant difference between predicted and observed percentages of signal below Nyquist. The observed percentages of the velocity profile at or below Nyquist frequency was highly correlated with the predicted percentages ($R^2 = 0.934$; $P = 0.007$; Table 2; Fig. 8).

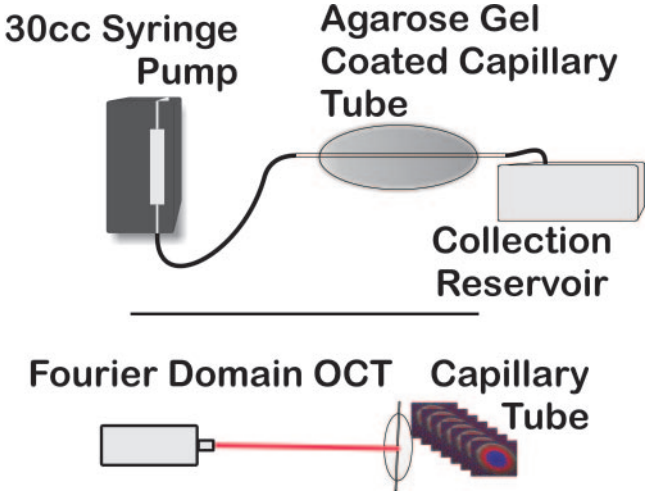

FIGURE 1. Skim milk was pumped at controlled rates from a 30-mL syringe pump, through a glass capillary tube embedded in a shallow bed of agarose gel, and was collected in a reservoir (*top*). The capillary tube was oriented at approximately 83° to the scanning beam. The 3D scan volume contained a series of axial slices acquired along the length of the capillary tube.

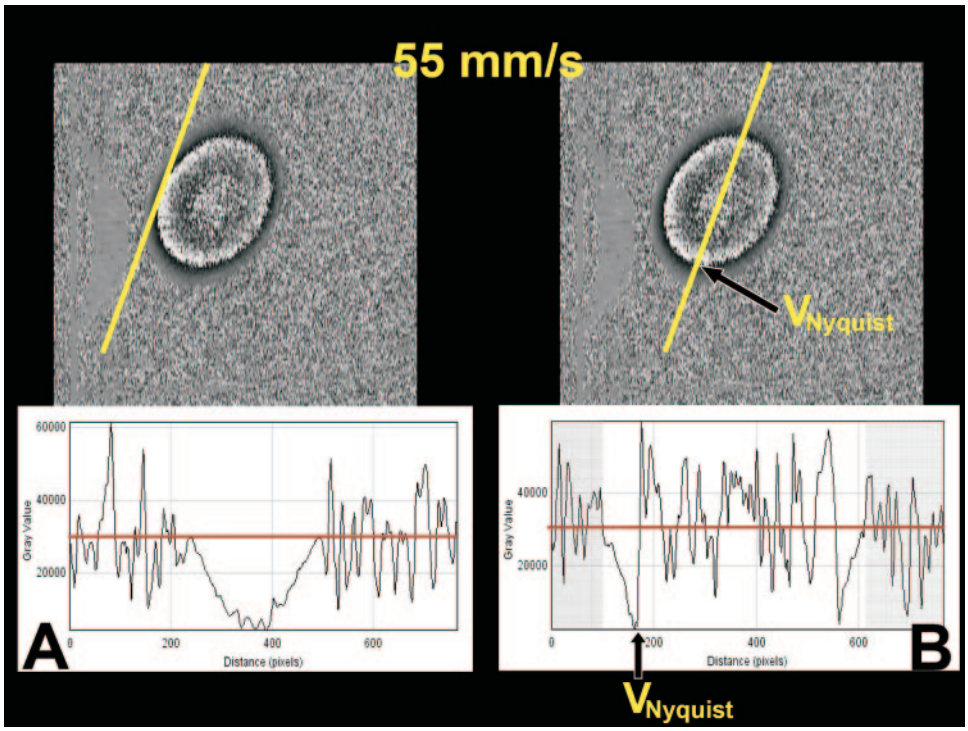

FIGURE 2. Velocity profiles at the location of Nyquist velocity (**A**) and through the center of the flow image. (**B**) Note the random appearance of Doppler signals within the phase-wrapped and fringe washout center velocities (**B**). *Yellow line*: location of velocity profile. *Red line*: level of 0 Doppler shift.

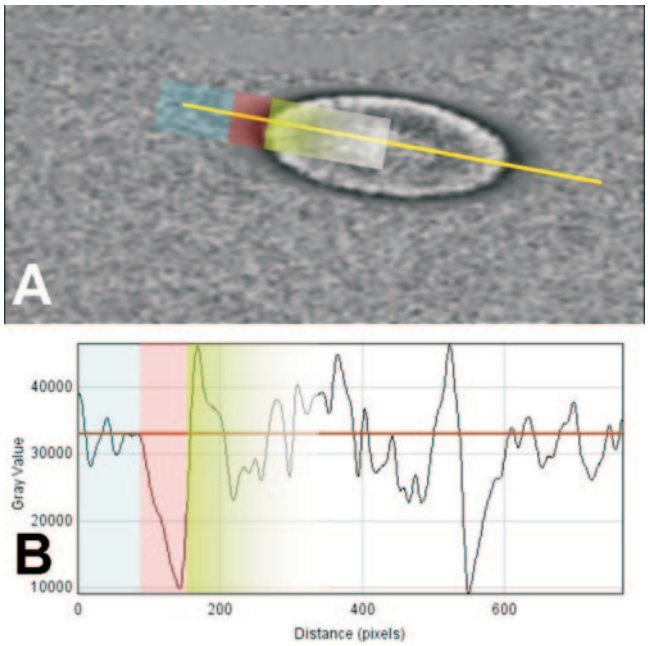

FIGURE 3. Examination of the Doppler signal (**A**) suggests that phase wrapped twice in this measurement, i.e., the maximum center velocity is greater than two times the Nyquist velocity. Smoothing failed to produce a velocity profile (**B**) that could accurately be measured. *Red line*: level of 0 Doppler shift. The region highlighted in *blue* is the background noise, consisting of random Doppler signals from the stationary glass tube. The region highlighted in *red* is the Doppler flow under and up to the Nyquist limit. The region fading from *green to white* is the flow signature beginning at a measureable level of phase wrapping but fading to noise because of fringe washout. The appearance of the light center suggests that a second Nyquist limit might have been passed; however, the noise observed in the velocity profile suggested that the signal degraded beyond a useful level.

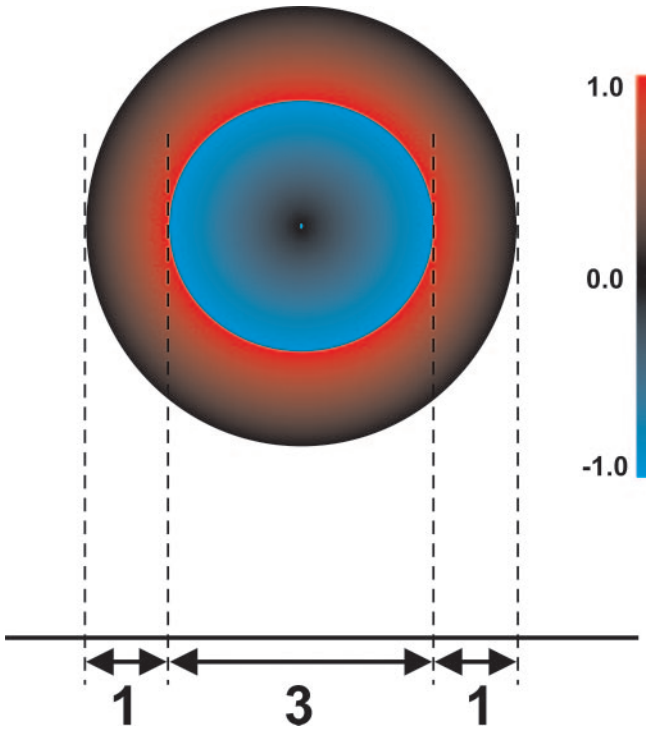

FIGURE 4. *Outer circle*: flow below the Nyquist limit. The portion of the velocity profile below Nyquist has a length of 2 (1+1), of a total length of 5 (1+3+1). Thus, 40% of the velocity profile occurs below the Nyquist limit. The predicted percentage of flow below Nyquist was used as the outcome parameter. The velocity profile (*bottom*) is obtained at the *yellow line*.

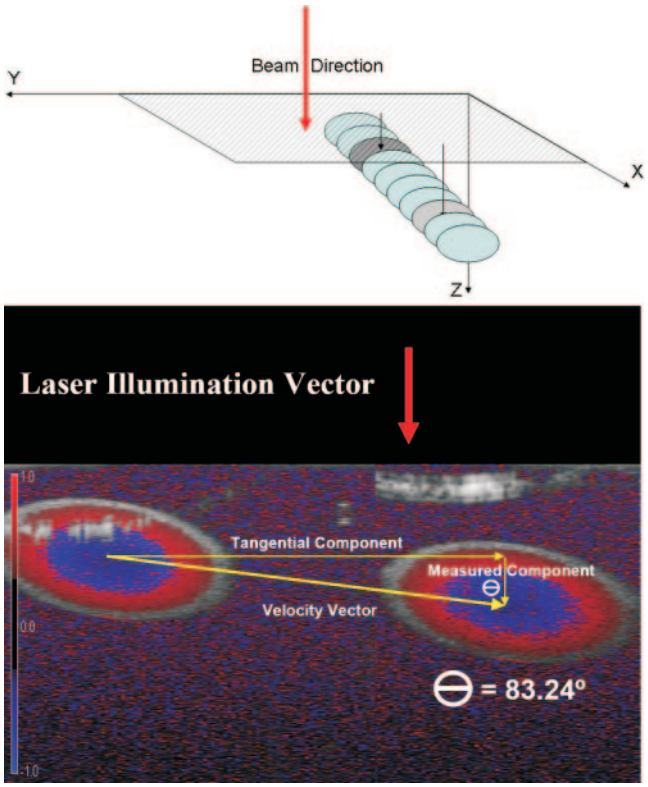

FIGURE 5. The position of the fluid column from two frames in the data set was superimposed onto a single image. The orientation of the tube velocity vector relative to the illuminating laser was computed, yielding a Doppler angle of 83.24°.

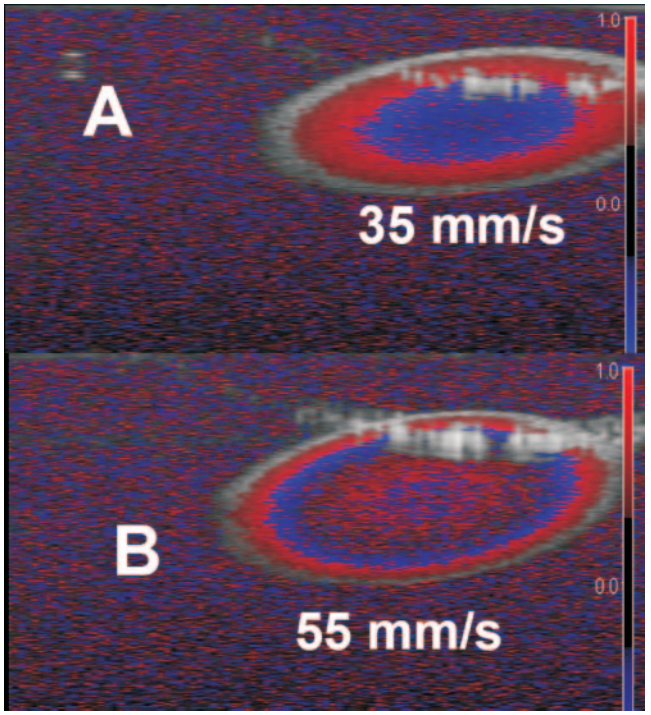

FIGURE 6. Fringe washout occurred in the experimental setup, resulting in the loss of signal from milk moving at velocities similar to those known to exist in the large vessels of the eye.

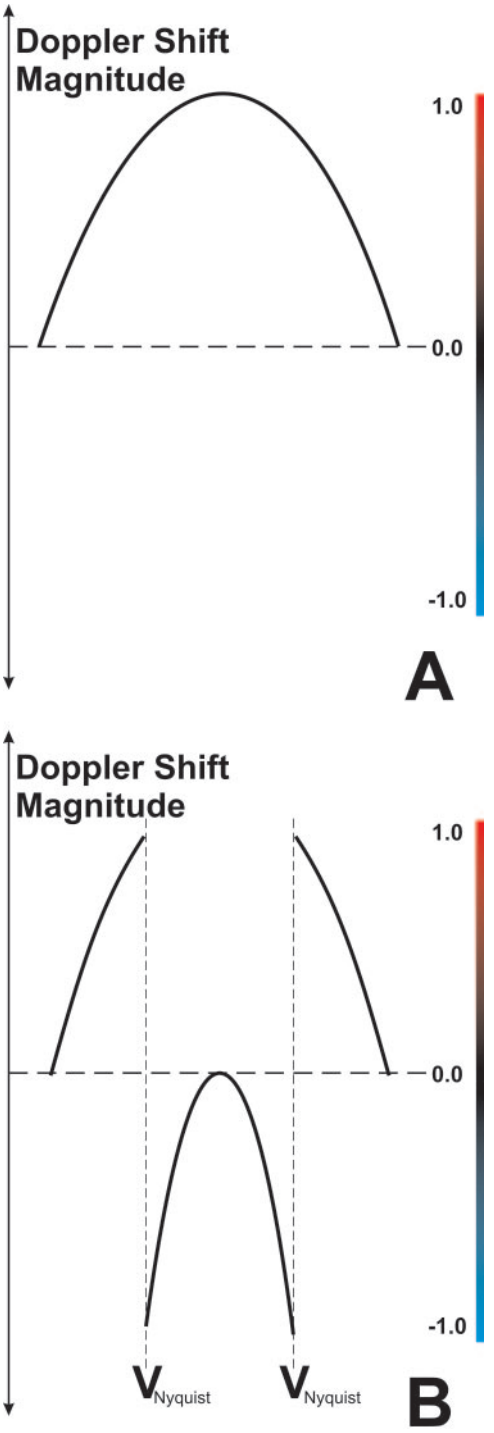

FIGURE 7. Under ideal conditions, Doppler signals would be below the Nyquist limit (**A**). If the Doppler signals exceeded the Nyquist limit (*arrows*), phase wrapping would occur, and a velocity pattern similar to (**B**) would be expected. *Red line*: level of 0 Doppler shift.

DISCUSSION

In the present study, we found that Doppler measurements, when performed within the measurement limits imposed by optical and scan parameters, were in excellent agreement with known values. However, as velocities increased above the Nyquist limit and phase wrapping was observed, fringe washout reduced reflectance and Doppler signals, resulting in the

degradation of Doppler signal to noise. It is possible to limit assessment to locations where flow is below Nyquist (Fig. 2A). Reflectance images display phase-wrapped flow as regions without observable reflective sources; thus, blood vessels typically present as black spaces in OCT images. Doppler images display phase-wrapped flow fields as areas containing stark black to white (or red to blue in color images) circles of transition surrounding a salt-and-pepper–appearing area of pure noise (Figs. 3, 6).

SD-OCT is capable of measuring Doppler shifts throughout each A-scan, but large Doppler shifts induce phase wrapping (Fig. 8).[5] Given laminar flow in the present study, it might appear that phase-unwrapping techniques could recover the actual velocity profile at velocities above the Nyquist limit.[7] However, progressive signal degradation after phase wrapping may prevent recovery of the true velocity signal. Within the fringe pattern, Doppler shifts physically manifest as lateral drift across the CCD within the spectrometer. Faster velocities produce larger Doppler shifts, resulting in faster drift. These drifts occur only within the frequency components associated with the location of the source of the Doppler shift, leaving other frequencies for the most part unaffected. If this drift is fast enough, fringe washout occurs.[8] Specifically, several peaks and troughs move across individual CCD pixels within the integration time of the camera, resulting in destructive interference and signal loss. This is why large blood vessels appear to be black within the center. The phase-unwrapping techniques referenced previously may be useful when Nyquist limit violations result in strong but erroneous signals. In SD-OCT Doppler measurements, however, excessively high Doppler shifts result in signal dropout, leaving only noise in the measurement.

It might also be thought that given valid velocity measurements in the low-velocity edge of the flow column, the actual flow distribution might be recovered by modeling the available accurate measurements to a parabolic flow distribution. This technique was used in the present study to predict the location in the flow column at which phase wrapping would occur. This technique is only applicable to biological systems if laminar flow is known to exist. When flow is laminar, the mean velocity is equal to half the v_{max}; the mean velocity in a turbulent flow system is equal to the mean. Studies of blood flow in glass tubes with diameters similar to those of retinal vasculature suggest that velocity was 1.6 times greater than the mean[9,10] and that flow in the retinal vasculature was neither purely laminar nor purely turbulent. Fitting measurements to a parabolic distribution would be invalid in either type of vessel.

The findings in the present study suggest that the current setting of SD-OCT is of limited use in biological systems. The Nyquist limit of 4.58 mm/s of the system used in this study is typical for SD-OCT configurations with available linear array camera technologies. This limit is far less than the peak arterial blood velocity in retinal arteries.[11] For arterial velocity to be scaled down by geometry (specifically the cosine term in the Doppler velocity equation) so as to be measurable by SD-OCT, the flow vector (the artery) would have to be oriented within approximately 4° perpendicular to the beam. However, setting of the present system is appropriate and useful for the measurement of very small velocities, as in retinal capillaries and aqueous drainage vasculature.

TABLE 2. Location of Nyquist Limit Velocity within Flow Tube as Calculated for All Flow Levels

Mean Velocity (mm/s)	Predicted Percentage below Nyquist	Observed Percentage below Nyquist
35.0	47.86	44.28
38.5	41.86	40.27
42.8	36.40	37.80
48.1	31.43	31.68
55.0	26.75	23.59

The percentage of total flow below the limit was compared with the observed flow below Nyquist. There was no statistically significant difference between observed and known levels.

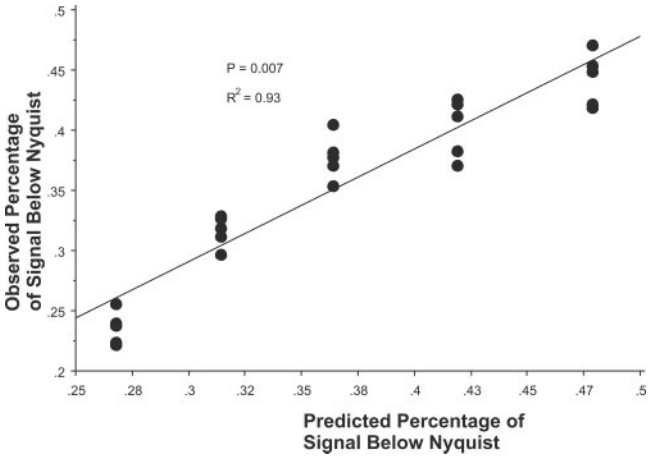

FIGURE 8. Observed and location of Nyquist level were highly correlated. *Solid line*: best-fit line.

In conclusion, SD-OCT provides objective Doppler measurements of laminar fluid flow in an in vitro flow system in a range up to the Nyquist limit. Efforts to obtain velocity measurements above the Nyquist limit may be impeded by the severe loss of data quality in the phase-wrapped range of velocities. These limits exclude measurements in large retinal vessels but allow accurate assessment of slow velocity systems such as retinal or anterior segment capillaries or the aqueous drainage system.

References

1. Huang D, Swanson EA, Lin CP, et al. Optical coherence tomography. *Science.* 1991;254:1178–1181.
2. Morgner U, Drexler W, Kartner FX, et al. Spectroscopic optical coherence tomography. *Opt Lett.* 2000;25:111–113.
3. Wojtkowski M, Leitgeb R, Kowalczyk A, Bajraszewski T, Fercher AF. In vivo human retinal imaging by Fourier domain optical coherence tomography. *J Biomed Opt.* 2002;7:457–463.
4. Bower BA, Zhao M, Zawadzki RJ, Izatt JA. Real-time spectral domain Doppler optical coherence tomography and investigation of human retinal vessel autoregulation. *J Biomed Opt.* 2007;12:041214.
5. Wang Y, Bower BA, Izatt JA, Tan O, Huang D. In vivo total retinal blood flow measurement by Fourier domain Doppler optical coherence tomography. *J Biomed Opt.* 2007;12:041215.
6. Leitgeb RA, Schmetterer L, Hitzenberger CK, et al. Real-time measurement of in vitro flow by Fourier-domain color Doppler optical coherence tomography. *Opt Lett.* 2004;29:171–173.
7. Fornaro G, Franceschetti G, Lanari R, Sansosti E. Robust phase-unwrapping techniques: a comparison. *J Opt Soc Am A.* 1996;13:2355–2366.
8. Yun SH, Tearney GJ, de Boer JF, Bouma BE. Motion artifacts in optical coherence tomography with frequency-domain ranging. *Opt Express.* 2008;12:2977–2998.
9. Damon DN, Duling BR. A comparison between mean blood velocities and center-line red cell velocities as measured with a mechanical image streaking velocitometer. *Microvasc Res.* 1979;17:330–332.
10. Baker M, Wayland H. On-line volume flow rate and velocity profile measurement for blood in microvessels. *Microvasc Res.* 1974;7:131–143.
11. Yoshida A, Feke GT, Mori F, et al. Reproducibility and clinical application of a newly developed stabilized retinal laser Doppler instrument. *Am J Ophthalmol.* 2003;135:356–361.